Inorganic Chemistry

Article

pubs.acs.org/IC

Temperature-Controlled Chiral and Achiral Copper Tetrazolate Metal–Organic Frameworks: Syntheses, Structures, and I_2 Adsorption

Ping Cui, Lijun Ren, Zhi Chen, Huancheng Hu, Bin Zhao,* Wei Shi, and Peng Cheng*

Department of Chemistry, Key Laboratory of Advanced Energy Material Chemistry, MOE, and TKL of Metal and Molecule Based Material Chemistry, Nankai University, Tianjin 300071, People's Republic of China

Supporting Information

ABSTRACT: Four tetrazole-based three-dimensional (3D) metal–organic frameworks (MOFs), $\{[Cu^{II}(btz)]\cdot 0.5H_2O\}_n$ (**1**), $[Cu^{II}(btz)]_n$ (**1′**), $\{[Cu^{II}(btz)]\cdot 0.5I_2\}_n$ (**1′·0.5I$_2$**), and $[Cu^{II}Cu^{I}_2(btz)_2]_n$ (**2**) [H_2btz = 1,5-bis(5-tetrazolo)-3-oxapentane)], have been successfully obtained and characterized by crystallography. Compound **1** features a chiral porous framework. The bulk crystallization of **1** is composed of enantiomers **1a** ($P4_1$) and **1b** ($P4_3$), which has been demonstrated by the crystal structure analyses of nine crystals of **1** randomly selected. The Cotton effect displayed in the solid-state circular dichroism spectrum of **1** is therefore attributed to enantiomeric excess rather than enantiopurity. The completely dehydrated phase of **1**, that is, **1′**, can adsorb 0.5 I_2 molecule per formula unit to yield compound **1′·0.5I$_2$**, which has been supported by single-crystal X-ray diffraction, elemental analysis, and thermogravimetric analysis. The locations of I_2 in the pores were unambiguously determined, and the interactions between I_2 molecules and the pore structures were investigated. Compound **2** crystallizes in an achiral $C2/c$ space group. Interestingly, the formations of chiral **1** and achiral **2** significantly depend on the reaction temperature. Between 80 and 140 °C, we got compound **1** as the only product. At 150 °C, both **1** and **2** were in coexistence in the final product. From 160 to 180 °C, only compound **2** was obtained. More interestingly, treatment of the crystals of **1** or the mixture of **1** and **2** obtained at 150 °C in their mother liquor at 170 °C yielded the crystals of **2** in a single phase.

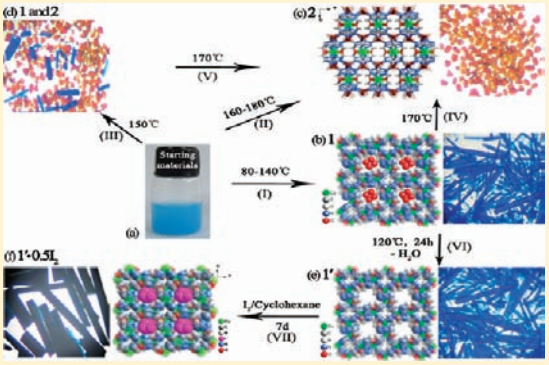

INTRODUCTION

Metal–organic frameworks (MOFs) with porous structures, as a unique class of crystalline solid-state materials, are rapidly investigated academically and industrially because of their pertinent applications.[1] Most of them focused on the adsorption and/or separation of guest molecules, for example, H_2, CH_4, CO_2, I_2, and the others.[1b,2,3] Among these studies, it has still been rather rare so far to determine the location of guest molecules within pores by single-crystal X-ray[4] or neutron diffraction techniques[5] owing to the following three aspects: (1) available neutron diffraction sources are very few in the whole world; (2) no single crystal is suitable for X-ray diffraction because of the loss of the crystalline state or the increasingly poor crystal quality after the adsorption of guest molecules; (3) more frequently, the serious disorder of guest molecules within pores causes the failure to determine their locations. Nevertheless, in order to better understand and improve the adsorption function of MOF materials, it is necessary to investigate the locations of the guest molecules within pores and the interactions between the guest molecules and pore structures.

On the other hand, MOFs associated with tetrazole and its derivatives have been developed rapidly because of their fascinating fuel gas or CO_2 storage, catalysis, nonlinear optics, molecular magnets, and luminescent properties.[6−9] For example, Xiong et al. adopted an in situ approach as a powerful strategy to design and construct tetrazole-based MOFs, displaying fluorescence, ferroelectric, dielectric, and second-order nonlinear optical properties.[6] Tetrazole-based MOFs with large channels for gas storage have also been reported by Long's group.[8] However, chiral porous MOFs built from tetrazole-based linkers are still rarely reported;[10] therefore, it is very meaningful to investigate their topologies and various functions. At present, the chiral MOFs are frequently designed and synthesized by using the chiral components as structure-directing agents, such as chiral organic linkers, chiral metal complexes, chiral templates, and so on.[11,12a] Although there are some reports on the employment of achiral precursors under spontaneous resolution to generate chiral MOFs, syntheses are still difficult because of the lack of predictability and tunability.[12]

In this contribution, four copper tetrazolates, namely, $\{[Cu^{II}(btz)]\cdot 0.5H_2O\}_n$ (**1**), $[Cu^{II}(btz)]_n$ (**1′**), $\{[Cu^{II}(btz)]\cdot 0.5I_2\}_n$ (**1′·0.5I$_2$**), and $[Cu^{II}Cu^{I}_2(btz)_2]_n$ (**2**) [H_2btz = 1,5-bis(5-tetrazolo)-3-oxapentane)], have been

Received: October 26, 2011
Published: January 30, 2012

   dx.doi.org/10.1021/ic2023105 | *Inorg. Chem.* 2012, 51, 2303–2310

Table 1. Crystallographic Data for Compounds 1a, 1b, 1′, 1′·0.5I_2, and 2

	1a	1b	1′	1′·0.5I_2	2
formula	$C_6H_9N_8O_{1.5}Cu$	$C_6H_9N_8O_{1.5}Cu$	$C_6H_8N_8OCu$	$C_6H_8N_8OICu$	$C_{12}H_{16}N_{16}O_2Cu_3$
fw	280.75	280.75	271.74	398.64	607.03
cryst syst	tetragonal	tetragonal	tetragonal	tetragonal	monoclinic
space group	$P4_1$	$P4_3$	$P4_1$	$P4_1$	$C2/m$
a (Å)	12.2996(3)	12.355(3)	12.3857(3)	12.3919(3)	7.5891(9)
b (Å)	12.2996(3)	12.355(3)	12.3857(3)	12.3919(3)	16.9978(18)
c (Å)	7.9073(3)	7.9025(16)	7.8956(3)	7.9043(3)	7.9254(13)
α (deg)	90	90	90	90	90
β (deg)	90	90	90	90	109.475
γ (deg)	90	90	90	90	90
V (Å^3)	1196.22(6)	1206.3(5)	1211.23(6)	1213.78(6)	963.9(2)
Z	4	4	4	4	2
D_{calcd} (g·cm^{-3})	1.559	1.546	1.490	2.182	2.092
Flack parameter	0.01(3)	0.00(2)	0.00(5)	0.00(5)	N/A
F(000)	568	568	548	760	606
θ range (deg)	3.06−25.00	2.33−27.87	3.06−24.98	3.06−25.01	2.40−24.99
reflns collected	2514	10066	2342	2285	2947
indep reflns	1876	2839	1389	1765	884
GOF on F^2	1.030	1.086	1.106	1.071	1.007
R1, wR2 [$I > 2\sigma(I)$]	0.0406, 0.1021	0.0390, 0.0995	0.0629, 0.1881	0.0775, 0.1988	0.0349, 0.0865
R1, wR2 (all data)	0.0471, 0.1045	0.0461, 0.1033	0.0709, 0.1974	0.0828, 0.2035	0.0421, 0.0884

successfully obtained. The formation of the chiral three-dimensional (3D) structure of **1** indicates that the conformational freedom of the achiral ligand H_2btz favors the formation of the helical structure. The formations and transformation studies of **1** and **2** suggest the importance of thermodynamic factors in the formation of two compounds. Taking the numerous nitrogen atoms exposed in the channel of **1** into account, the I_2-loading experiment was conducted and the locations of the I_2 molecules were clearly determined by single-crystal diffraction. Additionally, the optical activity and enantiomeric nature of **1**, **1′**, and **1′·0.5I_2** have also been investigated.

EXPERIMENTAL SECTION

Materials and General Methods. The H_2btz ligand was synthesized in advance according to the literature.[13] Solvents were rigorously dried before use. All other starting materials for syntheses were commercially purchased and used without further purification. The elemental analyses (C, H, and N) were carried out on a Perkin-Elmer elemental analyzer. The IR spectra were recorded on a Magna 750 FT-IR spectrophotometer with KBr pellets in the 4000−400 cm^{-1} region. The solid-state circular dichroism (CD) spectra were recorded on a Jasco J-750 spectropolarimeter using KBr pellets. The powder X-ray diffraction (PXRD) data were collected on a Rigaku D/Max-2500 diffractometer at 40 kV and 100 mA, employing a copper-target tube and a graphite monochromator. Thermogravimetric analyses (TGA) were performed on a Netzsch TG 209 TG-DTA analyzer under N_2 from room temperature to 800 °C at a heating rate of 2 °C·min^{-1} and an isotherm step at 270 °C for 2 h for compound **1′·0.5I_2** and at 10 °C·min^{-1} for compounds **1**, **1′**, and **2**.

Preparation of {[Cu^{II}(btz)]·0.5H_2O}$_n$ (1). $Cu(ClO_4)_2·6H_2O$ (0.0371 g, 0.1 mmol), H_2btz (0.0210 g, 0.1 mmol), H_2O (4 mL), and CH_3CH_2OH (2 mL) were sealed in a 25 mL Teflon-lined stainless steel autoclave and heated at 80−140 °C for 3 days. After cooling to room temperature at a rate of 1 °C·h^{-1}, blue needle crystals containing **1a** and **1b** were obtained. Yield: ca. 68% at 80 °C. Anal. Calcd for $C_6H_9N_8O_{1.5}Cu$: C, 25.67; H, 3.23; N, 39.91. Found: C, 25.45; H, 3.27; N, 39.42. Selected IR (KBr, cm^{-1}): 3569 (sb), 2943 (m), 2893 (m), 1668 (m), 1626 (w), 1503 (s), 1443 (vs), 1368 (s), 1265 (s), 1207 (s), 1113 (s), 1084 (vs), 1020 (s), 889 (m), 799 (m) cm^{-1}.

Preparation of [Cu^{II}(btz)]$_n$ (1′). Heating the as-synthesized crystals of **1** at 120 °C for 24 h afforded their desolvated phase (**1′**). Anal. Calcd for $C_6H_8N_8OCu$: C, 26.52; H, 2.97; N, 41.24. Found: C, 26.23; H, 3.16; N, 40.71. Selected IR (KBr, cm^{-1}): 2938 (m), 2891 (m), 1678 (m), 1624 (w), 1501 (s), 1443 (vs), 1368 (s), 1265 (s), 1211 (s), 1109 (s), 1082 (vs), 1022 (s), 891 (m), 799 (m) cm^{-1}.

Preparation of {[Cu^{II}(btz)]·0.5I_2}$_n$ (1′·0.5I_2). **1′** (0.0543 g, 0.2 mmol), I_2 (0.0355 g, 0.14 mmol), and cyclohexane (3.0 mL) were placed in a small sealed flask for 7 days at room temperature. The color of the crystals intensified from blue to dark blue, while their original crystallinity remained unchanged. The solution was decanted, and the resulting crystals were thoroughly washed with cyclohexane, collected, and dried in air. Yield: 0.0781 g corresponding to 0.47 I_2 being adsorbed per formula unit of **1′**. Anal. Calcd for $C_6H_8ON_8CuI$: C, 18.08; H, 2.02; N, 28.11. Found: C, 18.48; H, 2.42; N, 28.25. Selected IR (KBr, cm^{-1}): 3450 (w), 2938 (vw), 2893 (vw), 1626 (w), 1503 (m), 1443 (s), 1367 (w), 1265 (w), 1209 (m), 1113 (m), 1082 (s), 1022 (w), 889 (w), 798 (w) cm^{-1}.

Preparation of [Cu^{II}Cu$^{I}_2$(btz)$_2$]$_n$ (2). The same starting materials as those of **1** were sealed in a 25 mL Teflon-lined stainless steel autoclave and heated at 160−180 °C for 4 days. After cooling to room temperature at a rate of 1.5 °C·h^{-1}, brown crystals of **2** suitable for X-ray diffraction were obtained. Yield: ca. 42% at 160 °C. Anal. Calcd for $C_{12}H_{16}Cu_3N_{16}O_2$: C, 23.74; H, 2.66; N, 36.92. Found: C, 23.65; H, 2.87; N, 36.45. Selected IR (KBr, cm^{-1}): 3416 (w), 2926 (m), 2880 (m), 1640 (w), 1493 (s), 1418 (vs), 1364 (s), 1218 (m), 1107 (vs), 1038 (s), 894 (m) cm^{-1}.

Caution! *Owing to the potential explosive nature of tetrazole-based compounds, only a small amount of material should be used and handled with care!*

Crystal Structure Determination. Single-crystal X-ray diffraction measurements were carried out on an Oxford SuperNova TM diffractometer at 120(2) K (**1a**, **1′**, **1′·0.5I_2**, and **2**) and 293(2) K (**1.1−7**) and those of **1b** on a Rigaku Saturn 724 CCD diffractometer at 113(2) K. All diffractometers were equipped with graphite-monochromated Mo Kα radiation (λ = 0.710 73 Å), using the ω-scan technique for collections of the intensity data sets. Data reduction and empirical absorption corrections were applied with the *CrysAlis^{pro}* and *CrystalClear* software suites, respectively. All of the structures were solved by direct methods and refined anisotropically by full-matrix least-squares techniques based on F^2 using the *SHELXS-97* and *SHELXL-97* programs.[14] Anisotropic thermal parameters were

dx.doi.org/10.1021/ic2023105 | *Inorg. Chem.* 2012, 51, 2303−2310

assigned to all non-hydrogen atoms. The hydrogen atoms were placed in calculated positions in a riding model, and the isotropic displacement parameters were set to $1.2U_{eq}$ of the attached carbon atoms. Additionally, it should be noted that the structures have a large volume fraction of solvent-accessible voids (22.8% for **1.1**, 22.6% for **1.2**, 22.8% for **1.3**, 22.8% for **1.4**, 22.3% for **1.5**, 22.8% for **1.6**, and 22.6% for **1.7** per unit cell volume calculated by *PLATON* software[15]). The solvent molecules in those structures could not be crystallographically defined successfully, perhaps because of the heavy-disorder problem at single-crystal diffraction data collection (293 K). Pertinent crystallographic data and structural refinements for compounds **1a**, **1b**, **1′**, **1′·0.5I$_2$**, and **2** are summarized in Table 1. The selected bond lengths and angles of **1a**, **1b**, **1′**, **1′·0.5I$_2$**, and **2** with their estimated standard deviations are given in Table S1 in the Supporting Information.

RESULTS AND DISCUSSION

Selection of the Ligand. The ligand plays an essential role in constructing frameworks of crystalline solids.[16] The ligand H_2btz includes nine possible donor atoms (one oxygen and eight nitrogen atoms), which may not only coordinate to metal centers and but also interact with guest molecules. The H_2btz-containing MOFs may retain some uncoordinated atoms that can serve as exposed polarizing sites within the framework, giving rise to the potential utility as adsorption materials for guest molecules because of their strong binding interactions with the framework.

Description of Crystal Structures. *Crystal Structures of 1a, 1b, 1′, and 1′·0.5I$_2$.* Structure analyses reveal that **1a** and **1b** are enantiomers, crystallizing in two types of space groups, $P4_1$ and $P4_3$, respectively. Unfortunately, the pure crystals with only one conformation cannot be separated only by visualization. For compounds **1′** and **1′·0.5I$_2$**, their 3D frameworks are the same as that of **1a**. Compared to **1a**, no guest molecules exist in **1′** and I_2 instead of H_2O molecules are located in the channel of **1′·0.5I$_2$**. Here compound **1a** as a representative is described in detail. There are one crystallographically independent Cu^{2+} ion, one btz^{2-} ligand, and half of a guest H_2O molecule in an asymmetric unit (Figure 1). The

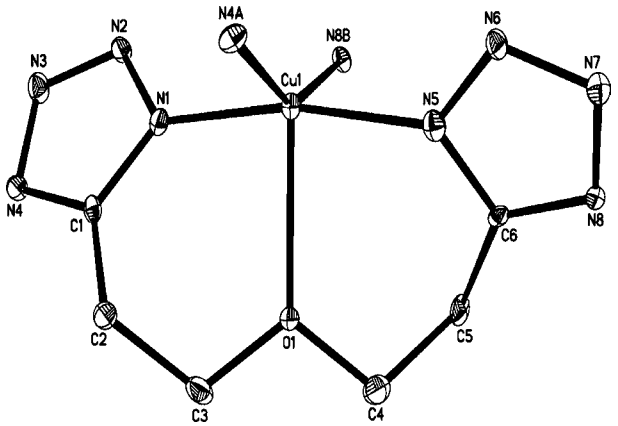

Figure 1. Coordination environment of the copper atom in **1a**, omitting hydrogen atoms and H_2O molecules for clarity.

five-coordinated Cu^{2+} ion resides in a distorted trigonal-bipyramidal geometry, coordinated by four nitrogen atoms (N1, N5, N4A, and N8B) and one oxygen atom (O1) from three btz^{2-} ligands. The Cu−N bond distances fall in the range of 1.934(5)−1.988(5) Å, and the Cu−O bond length is 2.326(4) Å, all of which are comparable to those reported previously.[17] In compound **1a**, each btz^{2-} ligand coordinates to three Cu^{2+} ions (model A, Scheme 1), and every tetrazolate

Scheme 1. Coordination Modes of Ligands Observed in Compounds 1a and 2

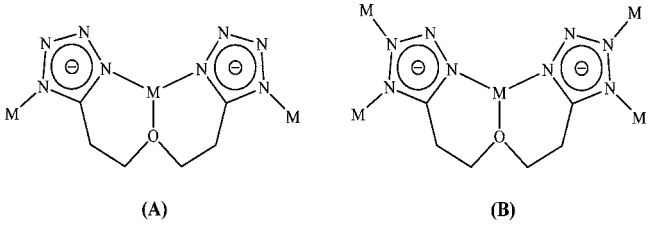

(Tz) ring bridges two Cu^{2+} ions in a μ_2-connected fashion with a coordination angle of ∼145° (Cu−Tz−Cu), quite analogous to that of imidazolate-ring-constructed zeolite nets.[18] The dihedral angle between two Tz rings of the btz^{2-} ligand is 113.9°.

The structure of compound **1a** features two types of one-dimensional (1D) channels along the crystallographic *c* axis, A and B (Figure 2a,b). Channel A has a large opening with a maximum diameter of 13.97 Å (atom-to-atom distance), in which free H_2O molecules are located. As shown in Figure 2c, the Tz rings constructing the walls of channel A exhibit two kinds of orientations, pointing toward and paralleling the *c* axis, while channel B has a quadrate cross section of approximately 8.89 × 8.89 or 5.31 × 5.31 Å^2 (atom-to-atom distance) along the diagonals or edges and a helical pitch of 7.91 Å (atom-to-atom distance) along the 4_1 screw axis. The key to the formation of this helical arrangement is attributable to the steric orientation of the Tz rings of the btz^{2-} ligand caused by the flexible O−$(CH_2CH_2-)_2$ spacer. Each A channel connects to four neighboring B channels, and each B channel also links with four A channels via sharing of their Tz rings containing N2 and N3 atoms, constructing a novel 3D chiral MOF. It is noteworthy that the uncoordinated nitrogen atoms, N2, N3, N6, and N7, are all exposed on the pore surfaces (Figure 2d). However, the N2 and N3 atoms are incapable of being as guest binding sites because of their lone electron pairs paralleling rather than pointing toward the channels. The lone electron pairs of the N6 and N7 atoms point into the channels, leading to a polar, strongly Lewis basic environment within the pores that is expected to encapsulate guest molecules. This can be confirmed by the short distance of the H_2O molecule with the N7 atom (O2···N7 = 3.084 Å). Upon solvent removal, open channels within the 3D framework are exploitable. The total solvent-accessible volume is approximately 21.9% calculated with *PLATON* software.

Furthermore, to gain a better insight into the nature of the framework structure, the network topology of **1a** is investigated. As described above, each mononuclear Cu^{2+} unit connects to four adjacent copper atoms via the Tz rings as linkers. Consequently, the 3D framework can be described as a 4-connected *unc* topology,[19a] with the Schläfli symbol of 6^6 and the vertex symbol of $6{\cdot}6{\cdot}6_2{\cdot}6_2{\cdot}6_3{\cdot}6_3$.[19b]

Crystal Structure of [Cu^{II}Cu$^{I}_2$(btz)$_2$]$_n$ (2). Crystals of **2** as a single phase were isolated by treatment of the same starting materials as those of **1** at 160−180 °C for 4 days. X-ray crystallography indicates that compound **2** crystallizes in the monoclinic space group *C*2/*m* and shows a 3D framework net, in which the coordination environments of the metal ions and

dx.doi.org/10.1021/ic2023105 | *Inorg. Chem.* 2012, 51, 2303−2310

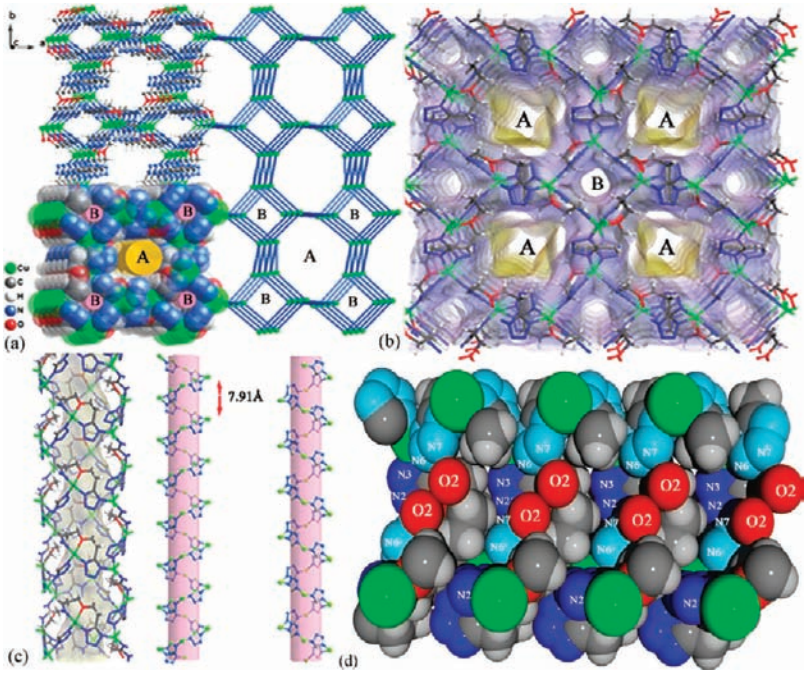

Figure 2. (a) View of the 3D structure along the *c* axis, exhibiting 1D nonhelical (A) and helical (B) channels. (b) Connolly surface (1.4 Å) of **1a** along the *c* axis. (c) Side view of the 1D nonhelical channel, right-handed helical chain in **1a**, and left-handed helical chain in **1b** along the *b* axis, respectively. The pitch is highlighted. (d) Locations of free H_2O molecules in the nonhelical channel obtained from the crystal structure.

bridging mode of the btz^{2-} ligand are shown in Figure 3. The asymmetric unit consists of one-quarter Cu^{2+} ion, half of a Cu^{+} ion, and half of the btz^{2-} ligand. Between the two crystallographically independent Cu^{2+} and Cu^{+} ions, the Cu^{+} ion displays a slightly distorted tetrahedral geometry coordinating to four nitrogen (N3, N3D, N4E, and N4F) atoms from four individual btz^{2-} ligands, while the six-coordinated Cu^{2+} ion is connected by four nitrogen (N1, N1A, N1B, and N1C) and two oxygen (O1 and O1A) atoms from two individual btz^{2-} ligands, affording four six-membered chelate rings that lock Cu^{2+} in a distorted octahedral geometry. The Cu–N bond distances are in the range of 2.009(3)–2.085(3) Å, which are in the normal ranges.[17b] The Cu–O distance of 2.620(3) Å is obviously longer, indicating the presence of a common Jahn–Teller effect of the Cu^{2+} ion. Each Tz ring is attached to two Cu^{+} and one Cu^{2+} ions, but each btz^{2-} ligand bridges one Cu^{2+} and four Cu^{+} ions because of the formation of the tridentate chelate bond (model B, Scheme 1). The dihedral angle between two Tz rings is 70.8° smaller than that of **1a**, which is apparently induced by their coordination fashion.

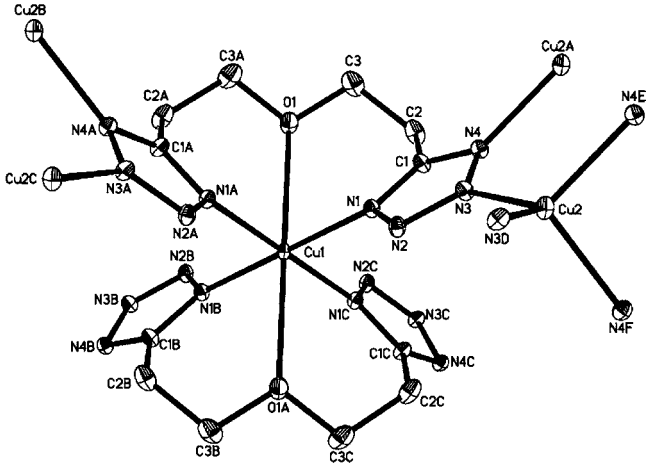

Figure 3. Coordination environments of the copper atoms in **2**, omitting hydrogen atoms for clarity.

Taking the structural feature of compound **2** into account, the framework becomes a (3,4,4)-connected topological net with the Schläfli symbol of $(4{\cdot}8^2)_4(4^2{\cdot}8^4)_2(8^4{\cdot}12^2)$ and the vertex symbol of $(4{\cdot}4{\cdot}8{\cdot}8{\cdot}8{\cdot}8)$ $(4{\cdot}8_2{\cdot}8_2)$ $(8_2{\cdot}8_2{\cdot}8_2{\cdot}8_2{\cdot}12_8{\cdot}12_8)$ (Figure 4), when Cu^{I} and Cu^{II} atoms are regarded as tetrahedral and square-planar 4-connected nodes, respectively, and the Tz rings are 3-connected nodes.

Effect of the Reaction Temperature on the Frameworks. The relationship between the formations of **1** and **2** and the synthetic temperatures is given from steps I to V in Figure 5. The 3D frameworks and crystal colors for **1**, **2**, **1′**, and **1′·0.5I₂** are presented in Figure 5b–f. The results reveal that the reaction temperature plays a crucial role in the formations of compounds **1** and **2**. By control of the temperature at 80, 100, 120, and 140 °C, respectively, only compound **1** was obtained in which the metal ions are all Cu^{2+} and the btz^{2-} ligand adopts the μ_3-bridging mode (step I). When the reaction temperature was applied at 160, 170, and 180 °C, respectively, compound **2** was isolated as the only product (step II). The framework structure of **2** is formed by the btz^{2-} ligand connecting to the Cu^{2+} and Cu^{+} ions in the μ_4-bridging mode. At 150 °C, **1** and **2** were in coexistence in the final product (step III). Further investigation showed that **1** can readily transform to **2**, when the crystals of **1** or the mixture of **1** and **2** obtained at 150 °C was placed in their mother liquor at the temperature 170 °C for 3 days (steps IV and V). The results mentioned above have been further confirmed by comparing PXRD with its corresponding simulated pattern (Figures 6 and 7). When the structure parameters of **1** are compared with those of **2** (Table 2), compound **2** has higher density packing.

dx.doi.org/10.1021/ic2023105 | *Inorg. Chem.* 2012, 51, 2303–2310

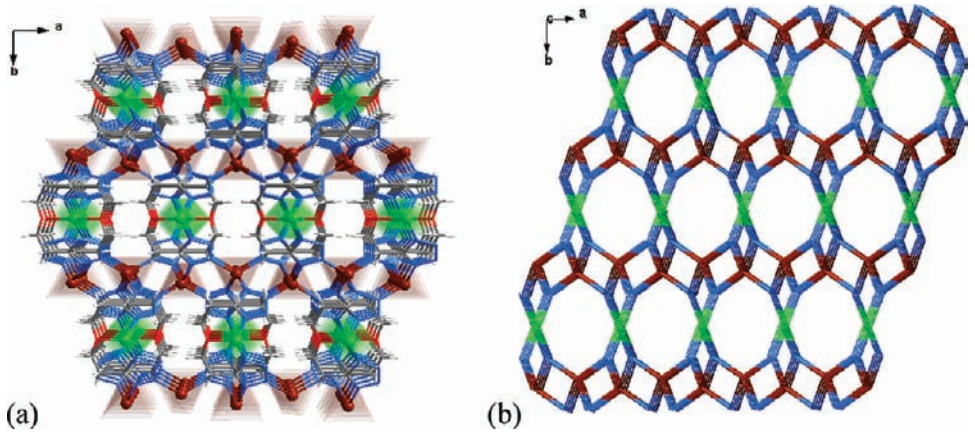

Figure 4. (a) View of the 3D framework of **2**. Color code: green, Cu^{2+}; dark red, Cu^{+}; red, O; gray, C; blue, N; white, H. (b) View of the 3D topology of **2**.

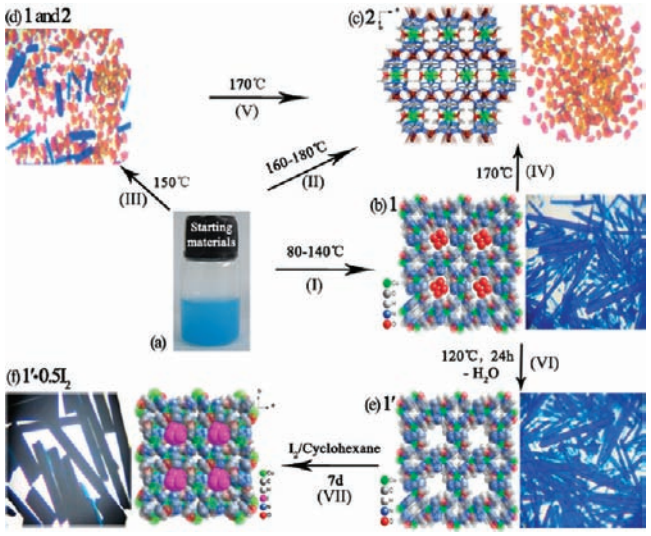

Figure 5. Relationship between the formations of **1** and **2** and the synthetic temperatures (steps I–V). Step VI stands for the crystal transformation from **1** to **1′** at 120 °C. Step VII suggests the process from **1′** to **1′·0.5I$_2$** by adsorbing I_2. The 3D frameworks and crystal colors for **1**, **2**, **1′**, and **1′·0.5I$_2$** are presented in parts b–f.

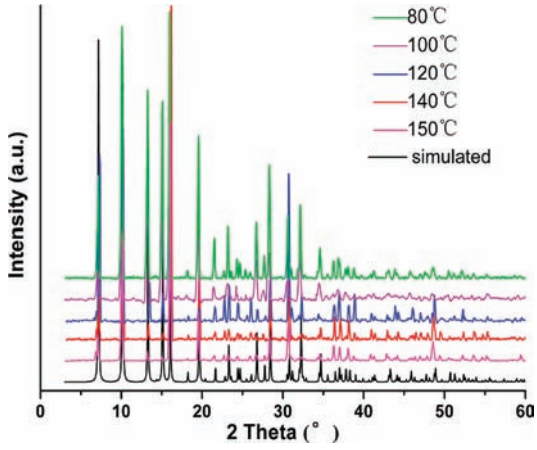

Figure 6. Comparison of the experimental PXRD patterns of as-synthesized **1** obtained at different reaction temperatures with the simulated diffraction pattern from the single-crystal X-ray data of **1a**.

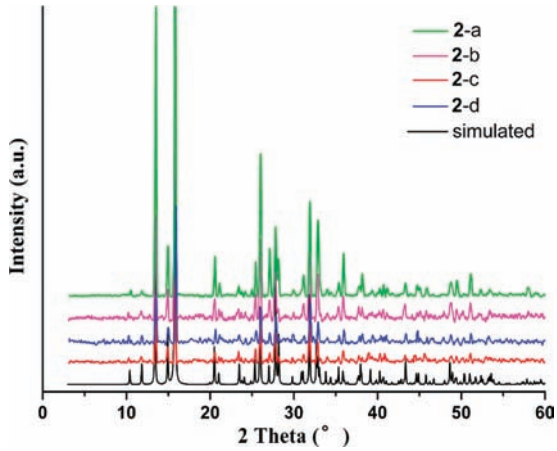

Figure 7. Experimental PXRD patterns of as-synthesized **2** under different conditions and the simulated diffraction pattern from its single-crystal X-ray data: **2**-a obtained at 160 °C; **2**-b obtained by heating **1** at 170 °C; **2**-c produced by heating the mixture of **1** and **2** at 170 °C; **2**-d picked from the mixture of **1** and **2** at 150 °C.

As a result, the framework of **2** is more stable than that of **1**, which is better confirmed by their TGA measurements (290 and 340 °C for **1** and **2**, respectively). All of the parameter changes are in accordance with the basic concept of the crystal growth under thermodynamic control.[20]

Adsorption and Location of I_2. The I_2-loading experiment was carried out for **1**. The result further demonstrates that there exists a void space in the framework. The crystals of **1** (0.0543 g) were heated at 120 °C for 24 h to afford the crystals of **1′** and then soaked in a solution of I_2 in cyclohexane for 7 days (steps VI and VII, Figure 5). The resulting crystals were thoroughly washed with cyclohexane to remove I_2 residing on the external surfaces of the crystals, and the mass increased by ca. 43.8 wt %, indicative of ~0.47 I_2 being adsorbed per the formula unit of **1′**, which was well consistent with the result of the single-crystal structure determination.

The locations of I_2 molecules are identified by single-crystal X-ray diffraction, and its formula is $\{[Cu(btz)]\cdot 0.5I_2\}_n$ (**1′·0.5I$_2$**), which is further confirmed by elemental analysis and TGA. The experimental PXRD pattern of **1′·0.5I$_2$** compared well with its simulated one, indicating the phase purity of the as-synthesized product (Figure S1 in the Supporting Information). Structurally, the I_2 molecules only

dx.doi.org/10.1021/ic2023105 | Inorg. Chem. 2012, 51, 2303–2310

Table 2. Comparison of Pertinent Parameters between Compounds 1a and 2

compound	space group (type)	V/Å^3, ρ_{calc}/(g·cm^{-3})	coordination mode of btz^{2-}	polymeric substructure
1a	noncentrosymmetric tetragonal ($P4_1$)	1196.22, 1.559	A	$[Cu^{II}(btz)]_n$ chiral 3D framework
2	centrosymmetric monoclinic ($C2/m$)	963.9, 2.092	B	$\{Cu^{II}Cu^{I}_2(btz)_2\}_n$ 3D framework

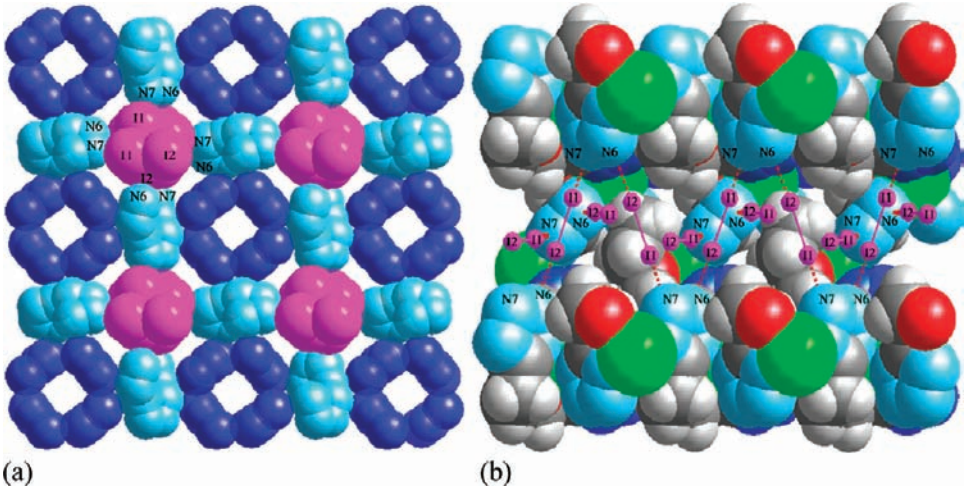

Figure 8. (a) Two kinds of orientations of the Tz rings, pointing toward (sky-blue) and paralleling (blue) the channels. (b) Locations of the I_2 molecules in **1′·0.5I$_2$** obtained from the crystal structure. The host framework is highlighted in a space-filling mode.

lie in the nonhelical channel, forming a chain in a head-to-tail fashion. The I–I bond length is 2.698(10) Å, in good agreement with those reported previously.[21] As for compound **1**, the Tz rings adopt two kinds of orientations, pointing toward and paralleling the *c* axis, and they may provide lone-electron and π-electron environments for the I_2 molecules, respectively (Figure 8). Compared to the sum of the van der Waals radii of iodine (2.15 Å) and nitrogen (1.55 Å), the short I···N distances of 3.046 and 3.399 Å indicate that there exit strong interactions between the I_2 molecules and nitrogen atoms of the Tz rings pointing toward the channels[21,22] (Figure S2 in the Supporting Information). Because the shortest distance between I_2 and the Tz rings paralleling the channels reaches 4.59 Å (I1···N1), there are no significant intermolecular interactions between them. Hence, compound **1′·0.5I$_2$** is clearly stabilized by donor–acceptor electrostatic attractions between the I_2 molecules and nitrogen atoms. Comparably, the interactions of I···H and I···C in the recent work published by Nenoff and co-workers were considered to play an important role in capturing and stabilizing I_2 molecules in cages.[21b] More importantly, the successful adsorption and location determination of the I_2 molecules may provide new insight for the design and application of MOF materials based on the Tz ligands.

CD Spectra. To confirm the optical activity and enantiomeric nature of **1**, **1′**, and **1′·0.5I$_2$**, the solid-state CD spectra were recorded on their single crystals from different batches, using pressed KBr pellets. The results of solid-state CD measurements display similar dichroic signals, a positive Cotton effect at 560 nm, and a negative Cotton effect at 700 nm (Figure 9). Therefore, whether losing the H_2O molecules of **1** or encapsulating the I_2 molecules of **1′**, the resulting **1′** and **1′·0.5I$_2$** retain their chirality. Meanwhile, the crystal structures of nine randomly picked crystals of **1** from the same reaction system have also been investigated. Seven of these crystals crystallize in the space group $P4_1$, and only two have a space group of $P4_3$, of which the Flack parameters are all near zero. Considering the crystal structures of nine crystals (Table 3), the

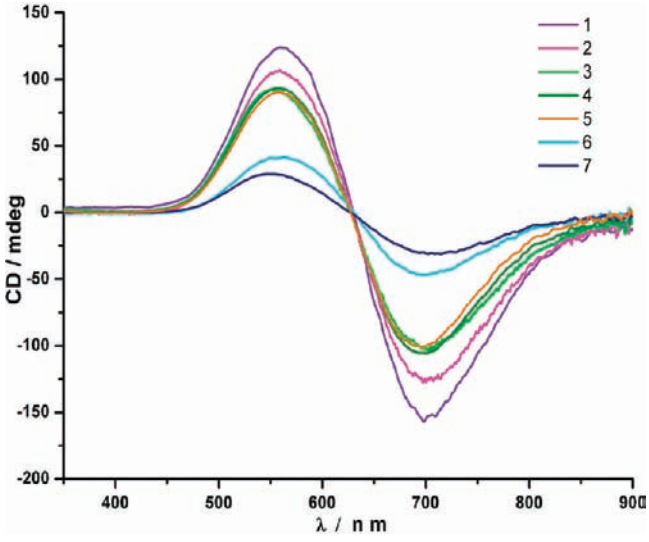

Figure 9. Solid-state CD spectra of **1** from three batches (curves 1–3), **1′** from two batches (curves 4 and 5), and **1′·0.5I$_2$** from two batches (curves 6 and 7).

bulk crystallization of **1** is confirmed to be enantiomeric excess rather than enantiopurity.

Because the H_2btz ligand is symmetric and there are no other driving forces to break the symmetry crystallization, such asymmetrical crystallization of the bulky sample from achiral precursors without any enantiopure sources is interesting. As we know, such similar examples are rarely reported.[7,23]

Thermal Stability Analyses. To confirm the thermal stabilities of the obtained bulk materials **1**, **1′**, **1′·0.5I$_2$**, and **2**, TGA were carried out (Figure 10). Compounds **1**, **1′**, and **1′·0.5I$_2$** show similar thermal stabilities because of their identical framework structures. The frameworks are stable up to about 290 °C for **1** and **1′** and 280 °C for **1′·0.5I$_2$**; further, a rapid weight loss is observed because of the explosive

dx.doi.org/10.1021/ic2023105 | Inorg. Chem. 2012, 51, 2303–2310

Table 3. Summary of the Structure Determinations of 1 (Nine Crystals), 1′, and 1′·0.5I_2 with the *R* Factors and Flack Absolute Structure Parameters for Each Refinement

	space group	*a*	*b*	*c*	R1	wR2	Flack parameter
1a	$P4_1$	12.2996(3)	12.2996(3)	7.9073(3)	0.0406	0.1045	0.01(3)
1b	$P4_3$	12.355(3)	12.355(3)	7.9025(16)	0.0390	0.0995	0.00(2)
1.1	$P4_1$	12.3879(3)	12.3879(3)	7.9323(3)	0.0401	0.1205	0.00(3)
1.2	$P4_1$	12.3684(2)	12.3684(2)	7.9094(2)	0.0376	0.1361	0.00(4)
1.3	$P4_1$	12.3965(3)	12.3965(3)	7.9197(3)	0.0395	0.1262	0.00(3)
1.4	$P4_1$	12.3933(3)	12.3933(3)	7.9318(3)	0.0486	0.1454	0.00(5)
1.5	$P4_1$	12.3494(16)	12.3494(16)	7.9086(10)	0.0723	0.1486	0.03(4)
1.6	$P4_1$	12.414(4)	12.414(4)	7.944(3)	0.0993	0.2069	0.00(7)
1.7	$P4_3$	12.3751(10)	12.3751(10)	7.9226(10)	0.0325	0.1180	0.00(3)
1′	$P4_1$	12.3857(3)	12.3857(3)	7.8956(3)	0.0629	0.1974	0.00(5)
1′·0.5I_2	$P4_1$	12.3919(3)	12.3919(3)	7.9043(3)	0.0775	0.2035	0.00(5)

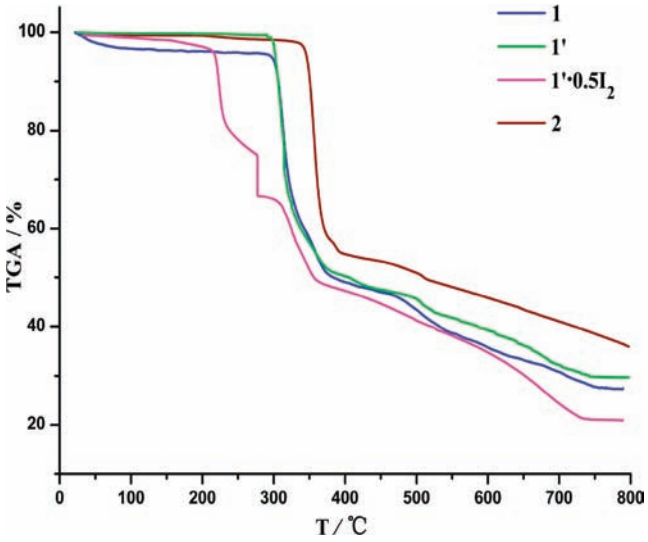

Figure 10. TGA plots of compounds **1**, **1′**, **1′·0.5I_2**, and **2** under a N_2 atmosphere.

combustion of btz^{2-} ligands. TGA for compound **1** displays a weight loss of 3.1% (calcd, 3.2%) in the range from room temperature to 80 °C, corresponding to the release of guest H_2O molecules. Decomposition of the residual components finally leads to the formation of CuO with a weight of 27.4% (calcd, 28.3%). There is no obvious weight loss before 290 °C in the TGA curve of compound **1′**. Beyond this temperature, a rapid weight loss is observed, leading to the formation of CuO as the residue (obsd, 29.9%; calcd, 29.3%). For **1′·0.5I_2**, removal of the I_2 molecules is in the range of 135−280 °C, which corresponds to half of a I_2 molecule (obsd, 33.3%; calcd, 31.8%). The final combusted residual composition is 21.1%, corresponding to the formation of CuO (calcd, 20.0%). As for compound **2**, it is stable up to about 340 °C. Upon further being heated, the 3D framework structure decomposes quickly because of the explosive combustion of the btz^{2-} ligands.

CONCLUSION

In summary, the relationship between the constructions of the tetrozole-based 3D MOFs and the synthetic temperatures was systematically investigated, indicative of significant temperature dependence in forming chiral **1** and achiral **2**, as well as in transforming **1** into **2**. The explorations on the CD spectra of **1** exhibit that the removal and change of the guest molecules in channels do not cause the disappearance of the Cotton signals, and noteworthily, the chirality of **1** derives from enantiomeric excess, which is unambiguously confirmed by determining the structures of many crystals of **1**. Importantly, the 3D framework in **1′** with two types of channels may absorb I_2 molecules to form **1′·0.5I_2**, and the locations of the guest I_2 molecules in **1′·0.5I_2** are structurally determined. The main stabilization of compound **1′·0.5I_2** is assigned to the strong donor−acceptor electrostatic attractions between the I_2 molecules and nitrogen atoms of the Tz rings.

ASSOCIATED CONTENT

Supporting Information

Crystallographic data in CIF format, table of selected bond lengths and angles for compounds **1a**, **1b**, **1′**, **1′·0.5I_2**, and **2**, and experimental and simulated PXRD patterns of **1′·0.5I_2**. This material is available free of charge via the Internet at http://pubs.acs.org.

AUTHOR INFORMATION

Corresponding Author

*E-mail: zhaobin@nankai.edu.cn (B.Z.), pcheng@nankai.edu.cn (P.C.).

ACKNOWLEDGMENTS

This work was supported by the 973 Program (Grants 2012CB821702 and 2011CB935902), NSFC (Grants 20971074 and 91122004), FANEDD (Grant 200732), and NSF of Tianjin (Grant 10JCZDJC21700).

REFERENCES

(1) (a) Lu, Z. Z.; Zhang, R.; Li, Y. Z.; Guo, Z. J.; Zheng, H. G. *J. Am. Chem. Soc.* **2011**, *133*, 4172−4174. (b) Li, J. R.; Ma, Y. G.; McCarthy, M. C.; Sculley, J.; Yu, J. M.; Jeong, H. K.; Balbuena, P. B.; Zhou, H. C. *Coord. Chem. Rev.* **2011**, *255*, 1791−1823. (c) Mu, W.; Liu, D. H.; Zhong, C. L. *Microporous Mesoporous Mater.* **2011**, *143*, 66−72. (d) Lee, J.; Farha, O. K.; Roberts, J.; Scheidt, K. A.; Nguyen, S. T.; Hupp, J. T. *Chem. Soc. Rev.* **2009**, *38*, 1450−1459. (e) Chang, N.; Gu, Z. Y.; Yan, X. P. *J. Am. Chem. Soc.* **2010**, *132*, 13645−13647.

(2) (a) Zeng, M. H.; Wang, Q. X.; Tan, Y. X.; Hu, S.; Zhao, H. X.; Long, L. S.; Kurmoo, M. *J. Am. Chem. Soc.* **2010**, *132*, 2561−2563. (b) Sun, D. F.; Ma, S. Q.; Ke, Y. X.; Collins, D. J.; Zhou, H. C. *J. Am. Chem. Soc.* **2006**, *128*, 3896−3897.

(3) (a) Chen, B. L.; Ockwig, N. W.; Fronczek, F. R.; Contreras, D. S.; Yaghi, O. M. *Inorg. Chem.* **2005**, *44*, 181−183. (b) Chen, B. L.; Xiang, S. C.; Qian, G. D. *Acc. Chem. Res.* **2010**, *43*, 1115−1124. (c) Xiang, S.; Zhang, Z.; Zhao, C. G.; Hong, K.; Zhao, X.; Ding, D. R.; Xie, M. H.; Wu, C. D.; Das, M. C.; Gill, R.; Thomas, K. M.; Chen, B. *Nat. Commun.* **2011**, *2*, 204.

(4) Vaidhyanathan, R.; Iremonger, S. S.; Shimizu, G. K. H.; Boyd, P. G.; Alavi, S.; Woo, T. K. *Science* **2010**, *330*, 650−653.
(5) (a) Peterson, V. K.; Liu, Y.; Brown, C. M.; Kepert, C. J. *J. Am. Chem. Soc.* **2006**, *128*, 15578−15579. (b) Dincă, M.; Dailly, A.; Liu, Y.; Brown, C. M.; Neumann, D. A.; Long, J. R. *J. Am. Chem. Soc.* **2006**, *128*, 16876−16883.
(6) (a) Zhao, H.; Qu, Z. R.; Ye, H. Y.; Xiong, R. G. *Chem. Soc. Rev.* **2008**, *37*, 84−100. (b) Cui, P.; Chen, Z.; Gao, D. L.; Zhao, B.; Shi, W.; Cheng, P. *Cryst. Growth Des.* **2010**, *10*, 4370−4378.
(7) Pachfule, P.; Chen, Y. F.; Sahoo, S. C.; Jiang, J. W.; Banerjee, R. *Chem. Mater.* **2011**, *23*, 2908−2916.
(8) (a) Horike, S.; Dincă, M.; Tamaki, K.; Long, J. R. *J. Am. Chem. Soc.* **2008**, *130*, 5854−5855. (b) Dincă, M.; Han, W. S.; Liu, Y.; Dailly, A.; Brown, C. M.; Long, J. R. *Angew. Chem., Int. Ed.* **2007**, *46*, 1419−1422. (c) Sumida, K.; Horike, S.; Kaye, S. S.; Herm, Z. R.; Queen, W. L.; Brown, C. M.; Grandjean, F.; Long, G. J.; Dailly, A.; Long, J. R. *Chem. Sci.* **2010**, *1*, 184−191.
(9) (a) Wu, T.; Yi, B. H.; Li, D. *Inorg. Chem.* **2005**, *44*, 4130−4132. (b) Li, M.; Li, Z.; Li, D. *Chem. Commun.* **2008**, 3390−3392. (c) Zhang, J. P.; Zhang, Y. B.; Lin, J. B.; Chen, X. M. *Chem. Rev.* **2012**, DOI: 10.1021/cr200139g.
(10) (a) Li, J. R.; Tao, Y.; Yu, Q.; Bu, X. H.; Sakamoto, H.; Kitagawa, S. *Chem.—Eur. J.* **2008**, *14*, 2771−2776. (b) Li, M. N.; Du, D. Y.; Yang, G. S.; Li, S. L.; Lan, Y. Q.; Shao, K. Z.; Qin, J. S.; Su, Z. M. *Cryst. Growth Des.* **2011**, *11*, 2510−2514. (c) Hu, T. P.; Bi, W. H.; Hu, X. Q.; Zhao, X. L.; Sun, D. F. *Cryst. Growth Des.* **2010**, *10*, 3324−3326.
(11) (a) Seo, J. S.; Whang, D.; Lee, H.; Jun, S. I.; Oh, J.; Jeon, Y. J.; Kim, K. *Nature* **2000**, *404*, 982−986. (b) Kesanli, B.; Lin, W. *Coord. Chem. Rev.* **2003**, *246*, 305−326.
(12) (a) Morris, R. E.; Bu, X. H. *Nat. Chem.* **2010**, *2*, 353−361. (b) Jiang, H. L.; Tsumori, N.; Xu, Q. *Inorg. Chem.* **2010**, *49*, 10001−10006.
(13) Chafin, A.; Irvin, D. J.; Mason, M. H.; Mason, S. L. *Tetrahedron Lett.* **2008**, *49*, 3823−3826.
(14) (a) Sheldrick, G. M. *SHELXL-97, Program for the Solution of Crystal Structures*; University of Gottingen: Gottingen, Germany, 1997. (b) Sheldrick, G. M. *SHELXL-97, Program for the Refinement of Crystal Structures*; University of Gottingen: Gottingen, Germany, 1997.
(15) Spek, A. L. *J. Appl. Crystallogr.* **2003**, *36*, 7−13.
(16) (a) Banerjee, R.; Phan, A.; Wang, B.; Knobler, C.; Furukawa, H.; O'Keeffe, M.; Yaghi, O. M. *Science* **2008**, *319*, 939−943. (b) Lin, J. B.; Zhang, J. P.; Chen, X. M. *J. Am. Chem. Soc.* **2010**, *132*, 6654−6656.
(17) (a) Tong, M. L.; Wu, Y. M.; Tong, Y. X.; Chen, X. M.; Chang, H. C.; Kitagawa, S. *Eur. J. Inorg. Chem.* **2003**, 2385−2388. (b) Zhang, X. M.; Zhao, Y. F.; Wu, H. S.; Batten, S. R.; Ng, S. W. *Dalton Trans.* **2006**, 3170−3178.
(18) Alkordi, M. H.; Brant, J. A.; Wojtas, L.; Kravtsov, V. Ch.; Cairns, A. J.; Eddaoudi, M. *J. Am. Chem. Soc.* **2009**, *131*, 17753−17755.
(19) (a) O'Keeffe, M.; Peskov, M. A.; Ramsden, S. J.; Yaghi, O. M. *Acc. Chem. Res.* **2008**, *41*, 1782−1789. (b) Blatov, V. A.; O'Keeffe, M.; Proserpio, D. M. *CrystEngComm* **2010**, *12*, 44−48.
(20) Rodriguez-Albelo, L. M.; Ruiz-Salvador, A. R.; Sampieri, A.; Lewis, D. W.; Gómez, A.; Nohra, B.; Mialane, P.; Marrot, J.; Sécheresse, F.; Mellot-Draznieks, C.; Biboum, R. N.; Keita, B.; Nadjo, L.; Dolbecq, A. *J. Am. Chem. Soc.* **2009**, *131*, 16078−16087.
(21) (a) Görbitz, C. H.; Nilsen, M.; Szeto, K.; Tangen, L. W. *Chem. Commun.* **2005**, 4288−4290. (b) Sava, D. F.; Rodriguez, M. A.; Chapman, K. W.; Chupas, P. J.; Greathouse, J. A.; Crozier, P. S.; Nenoff, T. M. *J. Am. Chem. Soc.* **2011**, *133*, 12398−12401.
(22) (a) Wang, Z. M.; Zhang, Y. J.; Liu, T.; Kurmoo, M.; Gao, S. *Adv. Funct. Mater.* **2007**, *17*, 1523−1536. (b) Choi, H. J.; Suh, M. P. *J. Am. Chem. Soc.* **2004**, *126*, 15844−15851. (c) Lu, J. Y.; Babb, A. M. *Chem. Commun.* **2003**, 1346−1347. (d) Hertzsch, T.; Budde, F.; Weber, E.; Hulliger, J. *Angew. Chem., Int. Ed.* **2002**, *41*, 2281−2284.
(23) Chen, S. C.; Zhang, J.; Yu, R. M.; Wu, X. Y.; Xie, Y. M.; Wang, F.; Lu, C. Z. *Chem. Commun.* **2010**, *46*, 1449−1451.